

SUSLOV PROBLEM WITH THE KLEBSH-TISSERAND POTENTIAL

SHENGDA HU, MANUELE SANTOPRETE

ABSTRACT. In this paper, we study a nonholonomic mechanical system, namely the Suslov problem with the Klebsh-Tisserand potential. We analyze the topology of the level sets defined by the integrals in two ways: using an explicit construction and as a consequence of the Poincaré-Hopf theorem. We describe the flow on such manifolds.

1. INTRODUCTION

A Hamiltonian system on a $2n$ -dimensional symplectic manifold is called completely integrable if it admits n independent integrals of motion in involution. For such systems, if the common level sets S_k of the integrals are compact, by the Liouville-Arnold theorem, the S_k are invariant tori of dimension n , and the flow on the tori is isomorphic to a linear flow. The system is super-integrable if there are more than n independent integrals of motions, and the invariant tori are of dimension less than n .

In the present paper, we are concerned with a family of dynamical systems, the so called Suslov's problem, that are not Hamiltonian, but exhibit important features of integrable and super-integrable Hamiltonian system. As first formulated in [6], it describes the dynamics of a rigid body with a fixed point immersed in a potential field and subject to a nonholonomic constraint that forces the angular velocity component along a given direction in the body to vanish. Our analysis shows that such systems have invariant tori carrying linear flows, as well as other types of invariant submanifolds carrying generically periodic flows.

The topology of invariant submanifolds of this problem have been studied by Tatarinov [7, 8] using surgery methods, and Fernandez-Bloch-Zenkov [2] using a generalization of the Poincaré-Hopf theorem to manifold with boundary together with some detailed information about the geometry of the problem. It was shown that the invariant submanifolds of this problems can be surfaces of genus between zero and five.

We will provide two further approaches for understanding the topology of the submanifolds, as well as the flows. The first is a direct construction that uses a Morse theoretic reasoning and in our opinion provides a better understanding of the geometry of the problem than the other approaches. The second is an application of the classical Poincaré-Hopf theorem for manifolds without boundary and requires only knowledge of the number of connected components of the manifold. Furthermore, we give a detailed analysis of the flow on the invariant submanifolds and find that, for certain values of the parameters, the system admits an additional integral of motion. The information thus obtained leads to concrete understanding of the physical motion of the problem.

Suslov's system is an example of an important class of nonholonomic systems, namely, the quasi-Chaplygin systems introduced in [1]. This system is Hamiltonizable in a very

precise sense, that we describe below. A non-holonomic system (Q, \mathcal{D}, L) consists of a configuration manifold Q , a Lagrangian $L : \mathcal{Q} \rightarrow \mathbb{R}$ and a non-integrable smooth distribution $\mathcal{D} \subset \mathcal{Q}$ describing kinematic constraints. The equations of motion are determined by the Lagrange-d'Alembert principle supplemented by the condition that the velocities are in \mathcal{D} , explicitly we have

$$(1.1) \quad \sum_{i=1}^n \left(\frac{\partial}{\partial \dot{x}_i} - \frac{d}{dt} \frac{\partial}{\partial \dot{x}_i} \right) \eta_i = 0, \quad \text{for all } \eta \in \mathcal{D}_x.$$

A **Chaplygin system** is a non-holonomic system (Q, \mathcal{D}, L) where Q has a principal bundle structure $Q \rightarrow \mathcal{Q}G$ with respect to a Lie group G , with a principal connection, and the distribution \mathcal{D} is the horizontal bundle of the connection. Therefore, given a vector $Y \in T_x Q$, we have the decomposition $Y = Y_h + Y_v$, with $Y_h \in \mathcal{D}_x$, and $Y_v \in \mathcal{V}_x$, where \mathcal{V} is the vertical bundle, and \mathcal{V}_x is the tangent space to the fiber at x . In addition one must require that the Lagrangian L is G -invariant.

A non-holonomic system is **quasi-Chaplygin** if, Q has a principal bundle structure $Q \rightarrow \mathcal{Q}G$ with respect to a Lie group G , but the connection is singular on some G -invariant subvariety $S \subset Q$, that is, for $x \in S$ the sum $\mathcal{D}_x + \mathcal{V}_x$ does not span the tangent space $T_x Q$. Quasi-Chaplygin systems can be regarded as usual Chaplygin systems in $Q \setminus S$, inside the set S , however, they behave differently (see [1]). It was shown in [1] that Suslov's problem is a quasi-Chaplygin system with $Q = \mathcal{S}^3$ (3) and $G = \mathcal{S}^1$ (2).

For Chaplygin systems the constrained Lagrangian $L_c(x, \dot{x}) = L(x, \dot{x}_h)$ induces a Lagrangian $l : \mathcal{M} \rightarrow \mathbb{R}$ via the identification $\mathcal{M} \approx \mathcal{D}/G$ (note that \mathcal{D}/G has the structure of a vector bundle with base space $\mathcal{Q}G$ and fiber \mathbb{R}^k , with $k = \dim(\mathcal{Q}G)$). Suppose the Legendre transform exists for l , which in local coordinates q on M is given by $(q, \dot{q}) \rightarrow (q, \frac{\partial l}{\partial \dot{q}})$. Under the Legendre transform, the system of equations (1.1) gives rise to a first order dynamical system on T^*M with corresponding vector field $X_{nh} = \{\cdot, H\}_{AP}$ for some function $H : T^*M \rightarrow \mathbb{R}$, where $\{\cdot, \cdot\}_{AP}$ is an almost Poisson bracket (i.e. a skew-symmetric bilinear operation on functions that satisfies the Leibniz identity but fails to satisfy the Jacobi identity). We say that the system is **Chaplygin Hamiltonizable**, if there is a nonvanishing function $f : \mathcal{Q}G \rightarrow \mathbb{R}$ such that

$$X_{nh} = f(q)X_H$$

with $X_H = \{\cdot, H\}$, and $\{\cdot, \cdot\} = \frac{1}{f} \{\cdot, \cdot\}_{AP}$ is a Poisson bracket.

For a quasi-Chaplygin system, if there is a function $f : \mathcal{Q}G \rightarrow \mathbb{R}$, nonvanishing in $Q \setminus S$, and such that $X_{nh} = f(q)X_H$ for some $H : T^*M \rightarrow \mathbb{R}$, we call the system **quasi-Chaplygin Hamiltonizable**. The Suslov problem considered in this article is quasi-Chaplygin Hamiltonizable with $f = \gamma_3$ ([1, 2]). For this type of systems, since the multiplier f has zeroes, one hypothesis of Theorem 1 in [4] fails and thus the topology of invariant manifolds may differ from tori. Here we give an explicit description of the invariant manifolds. We expect that the more explicit approach taken in this article may be able to shed light on more general quasi-Chaplygin Hamiltonizable systems.

The paper is organized as follows. In Section 2 we present an overview of the Suslov's problem in the Klebsh-Tisserand case. We give an elementary derivation of the equations of motion (see [1] for a derivation based on a Lagrangian approach). In Section 3 we give an explicit construction that allows us to determine the topology of the level surfaces S_k . Then, in Section 4 we study the flow of the system on the surfaces S_k , and we find that, for some parameter values there is one additional integral of motion. We then find and classify the critical points of the vector field. We use the Poincaré-Hopf theorem to give an alternative way to determine the topology of the surfaces. In Section 5 we use the topology of S_k and the results on the dynamics of the problem to describe how the rigid body moves in the three dimensional physical space.

2. SUSLOV'S PROBLEM WITH A KLEBSH-TISSERAND POTENTIAL

The Suslov problem describes the motion of a rigid body with a fixed point subject to a nonholonomic constraint. Wagner [9] suggested the following implementation of Suslov's model. He considered a rigid body, with a fixed point O , moving inside a spherical shell. The rigid body is attached at O with a spherical hinge so that it can turn around this point. The nonholonomic constraint is realized by considering two rigid caster wheels attached to the rigid body by a rod (see figure 1). These wheels force the angular velocity component along a direction orthogonal to the rod to vanish.

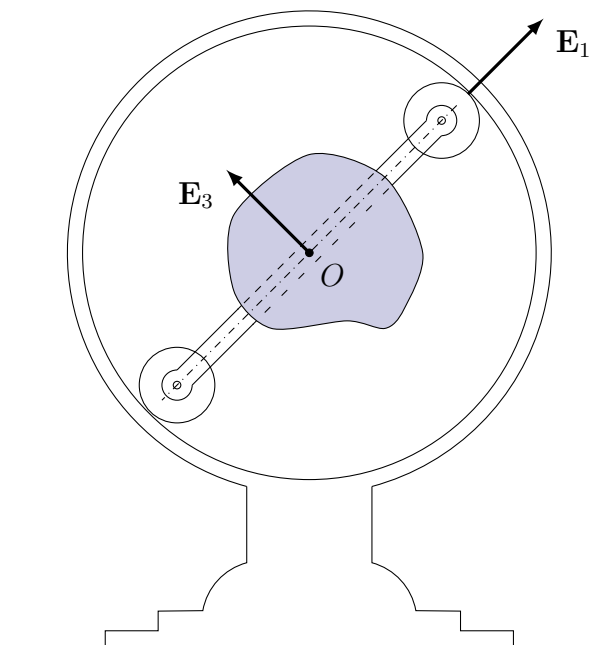


FIGURE 1. An implementation of the Suslov problem suggested by Wagner.

In this section we give an elementary derivation of the equations of motion for the Suslov's problem. These equations can also be obtained from a Lagrangian [1]. We begin by discussing the Euler equations for a rigid body without constraint. Denote

by $\{\mathbf{e}_1, \mathbf{e}_2, \mathbf{e}_3\}$ a right handed orthonormal basis of \mathbb{R}^3 , called the *spatial* frame. The coordinates of a point P in the spacial frame is denoted \mathbf{x} , which is also called the *spatial* vector of P . Let $\{\mathbf{E}_1, \mathbf{E}_2, \mathbf{E}_3\}$ be a right handed orthonormal frame, the *body* frame, defined by the three principal axis and let \mathbf{X} denote the *body* vector of the point P in this frame. We have

$$\mathbf{x} = \mathbf{R}\mathbf{X}, \text{ where } \mathbf{R} \text{ is a rotation matrix}$$

Let $\boldsymbol{\omega}$, $\boldsymbol{\pi}$ and $\boldsymbol{\tau}$ be the *spacial* vector of angular velocity, angular momentum, and torque, respectively. The corresponding *body* vectors are then given by

$$\boldsymbol{\Omega} = \mathbf{R}^{-1}\boldsymbol{\omega}, \boldsymbol{\Pi} = \mathbf{R}^{-1}\boldsymbol{\pi} \text{ and } \mathbf{T} = \mathbf{R}^{-1}\boldsymbol{\tau}$$

Note that if $\mathbb{I} = \text{diag}(I_1, I_2, I_3)$ denotes the body inertia tensor then we can also write $\boldsymbol{\Pi} = \mathbb{I}\boldsymbol{\Omega}$. Now $\boldsymbol{\tau} = \dot{\boldsymbol{\pi}}$, the second cardinal equation of dynamics, can be rewritten as

$$\mathbf{R}\mathbf{T} = \boldsymbol{\tau} = \frac{d}{dt}(\mathbf{R}\boldsymbol{\Pi}) = \dot{\mathbf{R}}\boldsymbol{\Pi} + \mathbf{R}\dot{\boldsymbol{\Pi}} \implies \dot{\boldsymbol{\Pi}} = -\mathbf{R}^{-1}\dot{\mathbf{R}}\boldsymbol{\Pi} + \mathbf{T}$$

Let $\hat{\boldsymbol{\Omega}} = \mathbf{R}^{-1}\dot{\mathbf{R}}$ be the *hat map*, then we have

$$\hat{\boldsymbol{\Omega}}\boldsymbol{\Pi} = \boldsymbol{\Omega} \times \boldsymbol{\Pi}$$

which gives

$$\dot{\boldsymbol{\Pi}} = \boldsymbol{\Pi} \times \boldsymbol{\Omega} + \mathbf{T}$$

Let $\boldsymbol{\alpha}$, $\boldsymbol{\beta}$, and $\boldsymbol{\gamma}$ be the body vectors of \mathbf{e}_1 , \mathbf{e}_2 , and \mathbf{e}_3 respectively, e.g.

$$\boldsymbol{\gamma} = \mathbf{R}^{-1}\mathbf{e}_3$$

Then we obviously have

$$\|\boldsymbol{\gamma}\|^2 = \gamma_1^2 + \gamma_2^2 + \gamma_3^2 = 1.$$

Suppose the rigid body is placed in a force field with potential energy

$$u(\mathbf{X}) = u(\langle \mathbf{X}, \boldsymbol{\gamma} \rangle),$$

where $\langle \cdot, \cdot \rangle$ is the Euclidean inner product. Then the total potential energy of the rigid body is

$$U(\boldsymbol{\gamma}) = \int_B u(\langle \mathbf{X}, \boldsymbol{\gamma} \rangle) d^3\mathbf{X}$$

and the total body force and torque are

$$\mathbf{F} = - \int_B \frac{\partial}{\partial \mathbf{X}} d^3\mathbf{X}, \quad \text{and } \mathbf{T} = - \int_B \frac{\partial}{\partial \mathbf{X}} \times \mathbf{X} d^3\mathbf{X},$$

respectively. We have

$$\frac{\partial}{\partial \mathbf{X}} \times \mathbf{X} = \frac{\partial}{\partial \langle \mathbf{X}, \boldsymbol{\gamma} \rangle} \frac{\partial \langle \mathbf{X}, \boldsymbol{\gamma} \rangle}{\partial \mathbf{X}} \times \mathbf{X} = - \left(\frac{\partial}{\partial \langle \mathbf{X}, \boldsymbol{\gamma} \rangle} \mathbf{X} \right) \times \boldsymbol{\gamma},$$

and similarly

$$\frac{\partial}{\partial \boldsymbol{\gamma}} = \frac{\partial}{\partial \langle \mathbf{X}, \boldsymbol{\gamma} \rangle} \frac{\partial \langle \mathbf{X}, \boldsymbol{\gamma} \rangle}{\partial \boldsymbol{\gamma}} = \frac{\partial}{\partial \langle \mathbf{X}, \boldsymbol{\gamma} \rangle} \mathbf{X}$$

which gives

$$\frac{\partial}{\partial \mathbf{X}} \times \mathbf{X} = - \frac{\partial}{\partial \boldsymbol{\gamma}} \times \boldsymbol{\gamma}.$$

Since γ does not depend on \mathbf{X} , integrating yields the following expression for the torque:

$$\mathbf{T} = \frac{\partial \mathcal{V}}{\partial \gamma} \times \gamma$$

and thus the dynamics equations are

$$\dot{\mathbf{\Pi}} = \mathbf{\Pi} \times \mathbf{\Omega} + \frac{\partial \mathcal{V}}{\partial \gamma} \times \gamma, \quad \dot{\gamma} = \gamma \times \mathbf{\Omega}$$

Let \mathbf{A} be a fixed unit body vector, and consider *Suslov's nonholonomic constraint*

$$\langle \mathbf{\Omega}, \mathbf{A} \rangle = 0$$

Subjecting the rigid body to this constraint is equivalent to adding a torque $\lambda \mathbf{A}$. The rigid body subject to this torque moves according to

$$\dot{\mathbf{\Pi}} = \mathbf{\Pi} \times \mathbf{\Omega} + \frac{\partial \mathcal{V}}{\partial \gamma} \times \gamma + \lambda \mathbf{A}, \quad \dot{\gamma} = \gamma \times \mathbf{\Omega}, \quad \langle \mathbf{\Omega}, \mathbf{A} \rangle = 0,$$

where the first equation can also be written as

$$(2.1) \quad \mathbb{I} \dot{\mathbf{\Omega}} = \mathbb{I} \mathbf{\Omega} \times \mathbf{\Omega} + \frac{\partial \mathcal{V}}{\partial \gamma} \times \gamma + \lambda \mathbf{A}.$$

Differentiating the constraint gives $\langle \mathbf{A}, \dot{\mathbf{\Omega}} \rangle = 0$, and substituting (2.1) into the constraint equation yields

$$\left\langle \mathbf{A}, \mathbb{I}^{-1} \left(\mathbb{I} \mathbf{\Omega} \times \mathbf{\Omega} + \frac{\partial \mathcal{V}}{\partial \gamma} \times \gamma + \lambda \mathbf{A} \right) \right\rangle = 0$$

and hence

$$\lambda = - \frac{\left\langle \mathbf{A}, \mathbb{I}^{-1} \left(\mathbb{I} \mathbf{\Omega} \times \mathbf{\Omega} + \frac{\partial \mathcal{V}}{\partial \gamma} \times \gamma \right) \right\rangle}{\langle \mathbf{A}, \mathbb{I}^{-1} \mathbf{A} \rangle}.$$

Let us consider the case $\mathbf{A} = \mathbf{E}_3$, so that the constraint is simply $\Omega_3 = 0$. Then the equation of the rigid body subject to Suslov's nonholonomic constraint are

$$I_1 \dot{\Omega}_1 = \gamma_2 \frac{\partial \mathcal{V}}{\partial \gamma_3} - \gamma_3 \frac{\partial \mathcal{V}}{\partial \gamma_2}, \quad I_2 \dot{\Omega}_2 = \gamma_3 \frac{\partial \mathcal{V}}{\partial \gamma_1} - \gamma_1 \frac{\partial \mathcal{V}}{\partial \gamma_3},$$

and

$$\dot{\gamma}_1 = -\gamma_3 \Omega_2, \quad \dot{\gamma}_2 = \gamma_3 \Omega_1, \quad \dot{\gamma}_3 = \gamma_1 \Omega_2 - \gamma_2 \Omega_1,$$

where we omitted the equation for $\dot{\Omega}_3$ since it is used only to determine λ and can be omitted. We consider the Klebsh-Tisserand case of the Suslov problem, i.e.

$$U(\gamma) = \frac{1}{2} (B_1 \gamma_1^2 + B_2 \gamma_2^2)$$

Then the equations of motion in terms of the momenta are given by

$$\begin{aligned}\dot{\Pi}_1 &= -B_2\gamma_2\gamma_3 \\ \dot{\Pi}_2 &= B_1\gamma_1\gamma_3 \\ \dot{\gamma}_1 &= -\gamma_3\frac{\Pi_2}{I_2} \\ \dot{\gamma}_2 &= \gamma_3\frac{\Pi_1}{I_1} \\ \dot{\gamma}_3 &= \gamma_1\frac{\Pi_2}{I_2} - \gamma_2\frac{\Pi_1}{I_1}.\end{aligned}$$

The following functions are easily seen to be integrals of motion of the equations above

$$F_1 := \frac{\Pi_1^2}{I_1} + B_2\gamma_2^2, \quad F_2 := \frac{\Pi_2^2}{I_2} + B_1\gamma_1^2.$$

Understanding of the Suslov problem now reduces to understanding of the flows on the level surfaces $F_1^{-1}(K_1) \cap F_2^{-1}(K_2)$ defined by the integrals of motion. It is convenient to perform the following change of variables:

$$m_1 = -\frac{\Pi_2}{I_2}, \quad b_1 = \frac{B_1}{I_2}, \quad k_1 = \frac{K_1}{I_2}; \quad m_2 = -\frac{\Pi_1}{I_1}, \quad b_2 = \frac{B_2}{I_1}, \quad k_2 = \frac{K_2}{I_1}.$$

and consider the system as defined in \mathbb{R}^5 , with coordinates $(m_1, m_2, \gamma_1, \gamma_2, \gamma_3)$, subject to the restriction

$$\gamma_1^2 + \gamma_2^2 + \gamma_3^2 = 1$$

Then the integrals of motion become $f_1 = m_1^2 + b_1\gamma_1^2$ and $f_2 = m_2^2 + b_2\gamma_2^2$. We write down the equations defining the level surfaces $S_k := f_1^{-1}(k_1) \cap f_2^{-1}(k_2)$:

$$(2.2) \quad \begin{cases} m_1^2 + b_1\gamma_1^2 = k_1 \\ m_2^2 + b_2\gamma_2^2 = k_2 \\ \gamma_1^2 + \gamma_2^2 + \gamma_3^2 = 1 \end{cases}$$

We also write the equations of motion in the new coordinates:

$$(2.3) \quad \begin{cases} \dot{m}_1 = -b_1\gamma_1\gamma_3 \\ \dot{m}_2 = b_2\gamma_2\gamma_3 \\ \dot{\gamma}_1 = m_1\gamma_3 \\ \dot{\gamma}_2 = -m_2\gamma_3 \\ \dot{\gamma}_3 = \gamma_2m_2 - \gamma_1m_1. \end{cases}$$

We denote by $X = (X_1, X_2, X_3, X_4, X_5) : \mathbb{R}^5 \rightarrow \mathbb{R}^5$, the vector field associated with the equations above.

3. TOPOLOGY OF THE LEVEL SURFACES S_k VIA AN EXPLICIT CONSTRUCTION

In this section we want to describe the topology of the level surfaces S_k by giving an explicit construction. Our method differs from the surgery approach pioneered by Tatarinov [7, 8]. Note that while it is difficult to find the original work of Tatarinov, an exposition of his method can be found in [3] and [2].

We start by finding the values of $k = (k_1, k_2)$ for which S_k is non-singular.

Lemma 3.1. *The subspace S_k is a smooth manifold of dimension 2 iff $k_1 k_2 \neq 0$ and all of the following holds: $k_1 \neq b_1$, $k_2 \neq b_2$ and $\frac{k_1}{b_1} + \frac{k_2}{b_2} \neq 1$.*

Proof. The matrix formed by the gradients of the defining equations is

$$(3.1) \quad 2 \begin{pmatrix} m_1 & 0 & b_1 \gamma_1 & 0 & 0 \\ 0 & m_2 & 0 & b_2 \gamma_2 & 0 \\ 0 & 0 & \gamma_1 & \gamma_2 & \gamma_3 \end{pmatrix}$$

and S_k is smooth iff matrix above to have maximal rank 3 at all points on S_k . Obviously, the matrix is of full rank when $m_1 m_2 \neq 0$; while it is degenerate when $k_1 k_2 = 0$.

For $m_1 = m_2 = 0$, we have, $b_1 \gamma_1^2 = k_1$ and $b_2 \gamma_2^2 = k_2$. It follows that

$$\gamma_3^2 = 1 - \frac{k_1}{b_1} - \frac{k_2}{b_2}$$

The rank 3 condition requires $\frac{k_1}{b_1} + \frac{k_2}{b_2} \neq 1$.

For $m_1 = 0$ but $m_2 \neq 0$, we have $b_1 \gamma_1^2 = k_1$. Rank 3 condition requires one of γ_2 or γ_3 is non-zero. We have $\gamma_2 = \gamma_3 = 0 \iff b_1 = k_1$, thus full rank implies $k_1 \neq b_1$.

The case $m_1 \neq 0$ but $m_2 = 0$ gives $k_2 \neq b_2$. \square

A simple consequence of the Lemma is that the topology of the level sets S_k can only change at values of k where S_k is singular. This is made precise in the following corollary.

Corollary 3.2. *The first quadrant in the (k_1, k_2) -plane is divided into 5 regions by*

$$k_1 = b_1, k_2 = b_2 \text{ and } \frac{k_1}{b_1} + \frac{k_2}{b_2} = 1$$

The subspace S_k has the same topological type for k in each region (c.f. Figure 2).

The level surfaces S_k are complete intersections. In (2.2), the first two equations define a 2-torus $T_k^2 \subset \mathbb{R}^4$, with coordinates $(m_1, m_2, \gamma_1, \gamma_2)$, while the last equation defines the unit 2-sphere $S^2 \subset \mathbb{R}^3$, with coordinates $(\gamma_1, \gamma_2, \gamma_3)$. It is therefore natural to study the level sets S_k by analyzing their projections onto these well understood surfaces. The projection onto the torus will be studied in the next subsection and it will be crucial in determining the topology of the level surfaces. The projection onto the unit 2-sphere S^2 will be studied in Subsection 5.1 to explain the connection between the topology of the S_k and the motion of the rigid body in physical space.

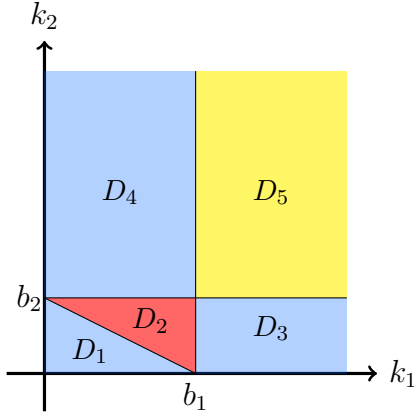


FIGURE 2. S_k is a smooth two-manifold (possibly disconnected) when (k_1, k_2) lies in the interiors of the shaded regions. For example, we will see that in the region D_5 shaded yellow, $S_k = 4S^2 = S^2 \sqcup S^2 \sqcup S^2 \sqcup S^2$.

3.1. Projection onto the torus. In order to describe the projection of the level surfaces S_k onto the 2-torus T_k^2 it is convenient to use a standard parametrization and describe the torus as the square flat torus. Since the first equation in (2.2) defines an ellipse in the (m_1, γ_1) -plane and the second equation defines an ellipse in the (m_2, γ_2) -plane, we parametrize these ellipses by the angle in the respective polar coordinates:

$$(3.2) \quad \begin{cases} m_1 = \sqrt{k_1} \cos \theta_1 \\ \gamma_1 = \sqrt{\frac{k_1}{b_1}} \sin \theta_1 \end{cases} \text{ and } \begin{cases} m_2 = \sqrt{k_2} \sin \theta_2 \\ \gamma_2 = \sqrt{\frac{k_2}{b_2}} \cos \theta_2 \end{cases}, \quad \theta_1 \in \left[-\frac{\pi}{2}, \frac{3\pi}{2}\right) \text{ and } \theta_2 \in [0, 2\pi)$$

Here the square $[-\frac{\pi}{2}, \frac{3\pi}{2}] \times [0, 2\pi]$ is viewed as the square flat torus T^2 by identifying the top side of the square with the bottom side, and the left side with the right side.

Then the parametrization above defines the following isomorphism from T_k^2 to the standard torus T^2 :

$$\varphi_k : T_k^2 \xrightarrow{\cong} T^2 : (m_1, m_2, \gamma_1, \gamma_2) \mapsto (\theta_1, \theta_2)$$

By definition, for each k , we see that $S_k \subset T_k^2 \times \mathbb{R}$, where the coordinate on the second factor is given by γ_3 . Let $p_k : S_k \rightarrow T_k^2$ be the projection induced by the projection of $T_k^2 \times \mathbb{R}$ to the first factor. The dependence of S_k on k can be described using $\varphi_k \circ p_k$.

To describe the projection of the surfaces S_k onto the torus (or more precisely the image of S_k under the map $\phi_k \circ p_k$) it is convenient to introduce the function $g_k : T^2 \rightarrow \mathbb{R}$ defined as

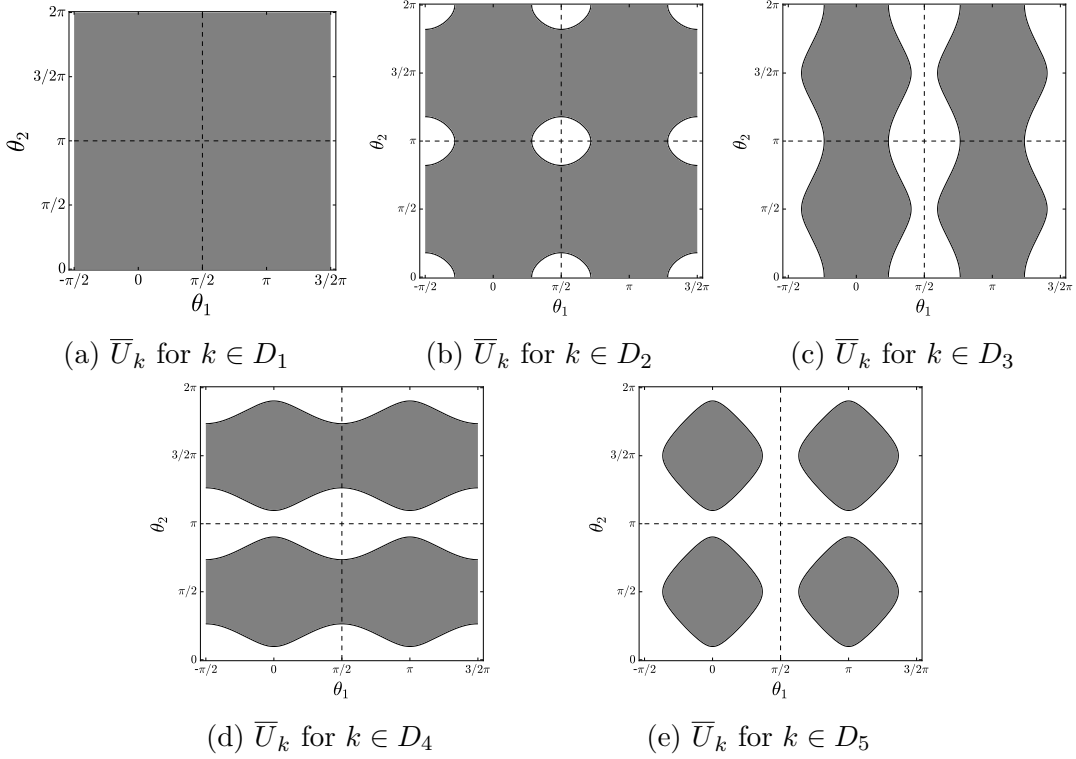
$$g_k(\theta_1, \theta_2) = \frac{k_1}{b_1} \cos^2 \theta_1 + \frac{k_2}{b_2} \sin^2 \theta_2$$

and let $k = (k_1, k_2)$. We denote by U_k the subset of T^2 consisting of all points at which g_k takes values greater than the real number ϵ_k , that is we set

$$U_k = \left\{ (\theta_1, \theta_2) \in T^2 : g_k > \epsilon_k = \frac{k_1}{b_1} + \frac{k_2}{b_2} - 1 \right\} \subseteq T^2$$

and let $\mathcal{D}_k = g_k^{-1}(\epsilon_k)$. Let $\bar{U}_k = U_k \cup \mathcal{D}_k$ be the closure of U_k . Figure 3 shows the set \bar{U}_k for various values of k .

The following Lemma shows that the set \bar{U}_k is the image of S_k under the map $\varphi_k \circ p_k$ and gives a characterization of such image.


 FIGURE 3. The set \bar{U}_k for various values of k .

Lemma 3.3. *For all k , we have $\bar{U}_k = \varphi_k \circ p_k(S_k)$. The map $\varphi_k \circ p_k : S_k \rightarrow \bar{U}_k$ is 2-to-1 over the interior U_k and is 1-to-1 over the boundary \mathcal{D}_k , if $\mathcal{D}_k \neq \emptyset$. Thus, S_k is homomorphic to the surface obtained by attaching two copies of \bar{U}_k along \mathcal{D}_k .*

Proof. The equation defining S_k in $T^2 \times \mathbb{R}$ is $\gamma_1^2 + \gamma_2^2 + \gamma_3^2 = 1$. It follows that $\varphi_k \circ p_k(S_k)$ is the subset of T^2 defined by

$$1 \geq \gamma_1^2 + \gamma_2^2 = \frac{k_1}{b_1} \sin^2 \theta_1 + \frac{k_2}{b_2} \cos^2 \theta_2$$

This is exactly \bar{U}_k . Over U_k , the strict inequality above holds, which implies that $\gamma_3 \neq 0$ takes 2 distinct values. It follows that $\varphi_k \circ p_k$ is 2-to-1 over U_k . Over the boundary \mathcal{D}_k , the equality holds and it implies that $\gamma_3 = 0$. Thus $\varphi_k \circ p_k$ is 1-to-1 along \mathcal{D}_k whenever it is not empty. \square

A consequence of this result is that we can use the shape of the set \bar{U}_k to characterize the geometry and the topology of the surfaces S_k . The following Lemma describes some feature of the function g_k that can be used to describe the shape of the sets \bar{U}_k .

Lemma 3.4. *The smooth function g_k on T^2 is a Morse function. The 16 critical points are independent of k , with 4 critical points on each of the 4 critical levels:*

- (1) *Minimums at $\left\{-\frac{\pi}{2}, \frac{\pi}{2}\right\} \times \{0, \pi\}$, with $g_k = 0$.*

- (2) Saddles at $\left\{-\frac{\pi}{2}, \frac{\pi}{2}\right\} \times \left\{\frac{\pi}{2}, \frac{3\pi}{2}\right\}$, with $g_k = \frac{k_1}{b_1}$.
- (3) Saddles at $\{0, \pi\} \times \{0, \pi\}$, with $g_k = \frac{k_2}{b_2}$.
- (4) Maximums at $\{0, \pi\} \times \left\{\frac{\pi}{2}, \frac{3\pi}{2}\right\}$, with $g_k = \frac{k_1}{b_1} + \frac{k_2}{b_2}$.

Proof. The statement follows from straightforward computations. \square

We can now use Lemmata 3.3 and 3.4 to completely characterize the surfaces S_k .

Proposition 3.5. *The topology of the surfaces S_k is described below:*

- For $k \in D_1$, S_k is isomorphic to two copies of T^2 .
- For $k \in D_2$, S_k is a genus 5 surface.
- For $k \in D_3$ or D_4 , S_k is isomorphic to two copies of T^2 .
- For $k \in D_5$, S_k is isomorphic to four copies of S^2 .

Proof. The results follow from understanding the set U_k using Lemma 3.4. For $k \in D_1$ we have $\frac{k_1}{b_1} + \frac{k_2}{b_2} < 1$, which gives $\varepsilon_k < 0$. Since $g_k \geq 0$, we see that $\mathcal{D}_k = \emptyset$, see Figure 3a. Thus S_k is isomorphic to two copies of T^2 .

For $k \in D_2$, we have

$$k_1 < b_1, k_2 < b_2, \frac{k_1}{b_1} + \frac{k_2}{b_2} > 1 \implies 0 < \varepsilon_k < \min \left\{ \frac{k_1}{b_1}, \frac{k_2}{b_2} \right\}$$

It follows by Lemma 3.4 that the set U_k is isomorphic to $T^2 \setminus 4D^2$, and $\mathcal{D}_k \cong 4S^1$, see Figure 3b. Lemma 3.3 implies that S_k is isomorphic to two copies of T^2 connect sum at 4 distinct points, i.e. a genus 5 surface.

For $k \in D_3$, we have

$$k_1 > b_1, k_2 < b_2 \implies \frac{k_2}{b_2} < \varepsilon_k < \frac{k_1}{b_1}$$

Then Lemma 3.4 implies that U_k consists of two components $C_{k,1} \cup C_{k,2}$, each of which is isomorphic to $S^1 \times (0, 1)$, and $\mathcal{D}_k \cong 4S^1$, see Figure 3c. Apply Lemma 3.3, we see that S_k has two components as well, each of which is isomorphic to a 2-torus. The argument for $k \in D_4$ is similar, where we have

$$k_1 < b_1, k_2 > b_2 \implies \frac{k_1}{b_1} < \varepsilon_k < \frac{k_2}{b_2}$$

and U_k again consists of two components, see Figure 3d. Again, S_k in this case has two components and each is isomorphic to a 2-torus.

For $k \in D_5$, we have

$$k_1 > b_1, k_2 > b_2 \implies \max \left\{ \frac{k_1}{b_1}, \frac{k_2}{b_2} \right\} < \varepsilon_k < \frac{k_1}{b_1} + \frac{k_2}{b_2}$$

Lemma 3.4 implies that U_k consists of 4 components $H_{k,j}$ for $j = 1, 2, 3, 4$, each of which is isomorphic to D^2 , the 2-disk, and $\mathcal{D}_k \cong 4S^1$, see Figure 3e. With Lemma 3.3, we find that S_k has four components, each of which is isomorphic to an S^2 . \square

4. DYNAMICS ON THE LEVEL SURFACES S_k

The projection to the torus as described in the previous section also provides us with detailed information on the Suslov flow.

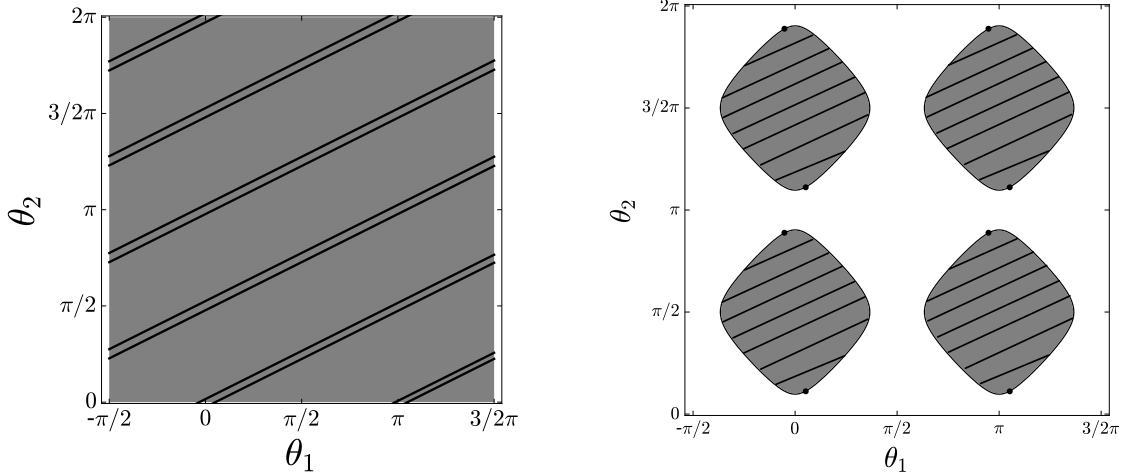
4.1. **Linear flow on tori.** We consider the region D_1 in Figure 2, where the level sets are two tori. From the proof of Proposition 3.5 each component of the level set at $(k_1, k_2) \in D_1$ is diffeomorphic to the torus in \mathbb{R}^4 with coordinates $(m_1, m_2, \gamma_1, \gamma_2)$ given by

$$\{m_1^2 + b_1\gamma_1^2 = k_1, m_2^2 + b_2\gamma_2^2 = k_2\}$$

Each equation above defines an ellipse in the plane, which, as we have seen, can be parametrized by introducing polar coordinates in each plane (3.2). In these coordinates, on the level surface, the Suslov flow (2.3) takes the form

$$\dot{\theta}_1 = \sqrt{b_1}\gamma_3, \quad \dot{\theta}_2 = \sqrt{b_2}\gamma_3$$

Thus the Suslov flow projects to a linear flow with slope $\sqrt{\frac{b_2}{b_1}}$ on the torus, which is periodic when the ratio is a rational number. On the square flat torus T^2 , the projected flow is given by pieces of straight lines with slope $\sqrt{\frac{b_2}{b_1}}$, see figure 4a.



(a) $b_1 = 4, b_2 = 1, k_1 = 1$, and $k_2 = 0.5$ (b) $b_1 = 4, b_2 = 1, k_1 = 4.4$, and $k_2 = 1.1$

FIGURE 4. (a) The flow for $k \in D_1$. In this case have rational slope $\sqrt{b_2/b_1} = 1/2$, and all the orbits are periodic. The picture shows four periodic orbits. (b) The flow for $k \in D_5$. There are 8 critical points. All the other orbits are periodic.

4.2. Additional integral of motion. When $\sqrt{\frac{b_2}{b_1}} \in \mathbb{Q}$ the system admits another integral of motion, which implies as well that Suslov flow on S_k is periodic for generic k in this case. We describe it first for $b_1 = b_2 = b$.

Proposition 4.1. *When $b_1 = b_2 = b$, the Suslov flow has the following as an integral of motion:*

$$f_3 = m_1 m_2 - b_1 \gamma_2$$

Proof. Straightforward verification by taking derivative with respect to t . \square

It's readily verified that the level sets of f_3 define the periodic flow on the tori for $k \in D_1$ when $b_1 = b_2$. In general, the new integral of motion is a higher degree polynomial in m_i 's and γ_i 's.

Proposition 4.2. *Suppose that the ratio $\sqrt{b_1} : \sqrt{b_2}$ is rational, then there is an integral of motion f_3 , given by a polynomial of $(\gamma_1, \gamma_2, m_1, m_2)$.*

Proof. For a given $k \in D_1$, rewrite the flow equations (2.3) in the (θ_1, θ_2) -coordinates:

$$\begin{cases} m_1 = \sqrt{k_1} \cos \theta_1 \\ \gamma_1 = \sqrt{\frac{k_1}{b_1}} \sin \theta_1 \end{cases} \text{ and } \begin{cases} m_2 = \sqrt{k_2} \sin \theta_2 \\ \gamma_2 = \sqrt{\frac{k_2}{b_2}} \cos \theta_2 \end{cases}$$

where $-\frac{\pi}{2} \leq \theta_1 \leq \frac{3\pi}{2}$ and $0 \leq \theta_2 \leq 2\pi$, and we have

$$\dot{\theta}_1 = \sqrt{b_1} \gamma_3, \dot{\theta}_2 = \sqrt{b_2} \gamma_3$$

Let $p, q \in \mathbb{Z}$ be integers such that

$$\sqrt{\frac{b_1}{b_2}} = \frac{p}{q}$$

then we see that $\theta_1 - \theta_2$ is a constant along the flow

$$q\dot{\theta}_1 - p\dot{\theta}_2 = (q\sqrt{b_1} - p\sqrt{b_2})\gamma_3 = 0$$

Furthermore, we can express trigonometric functions of $\theta_1 - \theta_2$ as a degree $p + q$ polynomial in $m_1, m_2, \gamma_1, \gamma_2$, involving also k_1 and k_2 . For example, let $z_1 = e^{i\theta_1}$ and $z_2 = e^{i\theta_2}$, then

$$\cos(\theta_1 - \theta_2) = \Re(z_1^q z_2^{-p}) = \Re((\cos \theta_1 + i \sin \theta_1)^q (\cos \theta_2 - i \sin \theta_2)^p)$$

It follows that

$$f_3 = \Re \left((m_1 + i\sqrt{b_1}\gamma_1)^q (\sqrt{b_2}\gamma_2 - im_2)^p \right) = k_1^{\frac{q}{2}} k_2^{\frac{p}{2}} \cos(\theta_1 - \theta_2)$$

is a constant along the flows for $k \in D_1$. It is straightforward to verify by direct differentiation that $(m_1 + i\sqrt{b_1}\gamma_1)^q (\sqrt{b_2}\gamma_2 - im_2)^p$ is a constant along the flow independent of k . Thus f_3 is an integral of motion, which is a degree $p + q$ real polynomial in $(\gamma_1, \gamma_2, m_1, m_2)$. \square

4.3. Critical Points. Critical points of the flow of the Suslov problem can be obtained by a simple geometric argument. We observe that the critical points are precisely where the level sets \mathcal{D}_k are tangent to the linear flow. Thus, in (θ_1, θ_2) coordinates, the critical points are exactly the solutions to the following system of equations:

$$\begin{aligned} \frac{k_1}{b_1} \sin^2 \theta_1 + \frac{k_2}{b_2} \cos^2 \theta_2 &= 1 \\ \frac{k_1 b_2 \sin \theta_1 \cos \theta_1}{b_1 k_2 \sin \theta_2 \cos \theta_2} &= \sqrt{\frac{b_2}{b_1}} \end{aligned}$$

The second equation simplifies to

$$\frac{k_1^2}{b_1} \sin^2 \theta_1 (1 - \sin^2 \theta_1) = \frac{k_2^2}{b_2} (1 - \cos^2 \theta_2) \cos^2 \theta_2$$

Using the first equation and the fact that $\gamma_1^2 = \frac{k_1}{b_1} \sin^2 \theta_1$, we obtain the following quadratic equation in γ_1^2 , which can be explicitly solved:

$$(4.1) \quad (b_1 - b_2)\gamma_1^4 - (k_1 + k_2 - 2b_2)\gamma_1^2 + (k_2 - b_2) = 0.$$

When $b_1 = b_2 := b$, (4.1) reduces to

$$(k_1 + k_2 - 2b)\gamma_1^2 + (k_2 - b) = 0 \implies \gamma_1 = \pm\gamma_1^*, \text{ where } \gamma_1^* = \sqrt{\frac{k_2 - b}{k_1 + k_2 - 2b}}$$

Let

$$\gamma_2^* = \sqrt{\frac{k_1 - b}{k_1 + k_2 - 2b}} \text{ and } t = \sqrt{k_1 + k_2 - b}$$

then the critical points in this case are given in Table 1 below:

Region	Value of Parameters	# of cp	critical points: $(m_1, m_2, \gamma_1, \gamma_2, \gamma_3)$
D_1	$k_1 + k_2 < b$	0	
D_2	$k_1 + k_2 > b, k_1 < b, k_2 < b$	8	$\pm(\pm t\gamma_2^*, \pm t\gamma_1^*, \pm\gamma_1^*, \pm\gamma_2^*, 0),$ $\pm(\pm t\gamma_2^*, \mp t\gamma_1^*, \mp\gamma_1^*, \pm\gamma_2^*, 0)$
D_3	$k_1 > b, k_2 < b$	0	
D_4	$k_1 < b, k_2 > b$	0	
D_5	$k_1 > b, k_2 > b$	8	$\pm(\pm t\gamma_2^*, \pm t\gamma_1^*, \pm\gamma_1^*, \pm\gamma_2^*, 0),$ $\pm(\pm t\gamma_2^*, \mp t\gamma_1^*, \mp\gamma_1^*, \pm\gamma_2^*, 0)$

TABLE 1. Critical points for $b_1 = b_2$. See Figure 2 for a definition of the regions D_i .

Suppose that $b_1 \neq b_2$. As a quadratic equation in γ_1^2 , the discriminant of (4.1) is

$$(4.2) \quad \Delta = (k_1 + k_2 - 2b_2)^2 - 4(b_1 - b_2)(k_2 - b_2)$$

The solutions of equation (4.1) are $\gamma_1 = \pm\Gamma_1^-, \pm\Gamma_1^+$ with

$$(4.3) \quad \Gamma_1^- = \sqrt{\frac{(k_1 + k_2 - 2b_2) - \sqrt{\Delta}}{2(b_1 - b_2)}}, \Gamma_1^+ = \sqrt{\frac{(k_1 + k_2 - 2b_2) + \sqrt{\Delta}}{2(b_1 - b_2)}}$$

which can be real or complex depending on the value of the parameters.

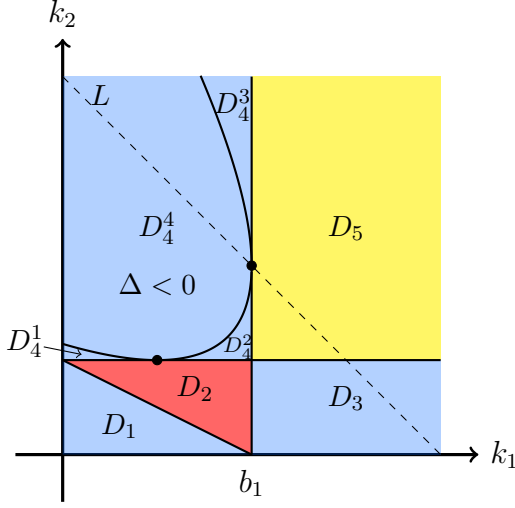


FIGURE 5. The curve $\Delta = 0$ divides the region D_4 into four subregions, namely, D_4^1 , D_4^2 , D_4^3 , and D_4^4 , where D_4^4 is the subregion where $\Delta < 0$. The equation for the dashed line L is $k_1 + k_2 = 2b_1$. We denote with C_1 the part of $\Delta = 0$ below the line L and with C_2 the part above L .

It's straightforward to see, from (4.3), that there are no critical points in D_4^4 . Let

$$\Gamma_2^\pm = \sqrt{1 - (\Gamma_1^\pm)^2}, \Lambda_1^\pm = \sqrt{k_1 - b_1(\Gamma_1^\pm)^2} \text{ and } \Lambda_2^\pm = \sqrt{k_2 - b_2(\Gamma_2^\pm)^2}$$

We can then describe the critical points for $b_1 > b_2$ in Table 2 below, where the regions are as labeled in Figure 5.

Region	Value of Parameters		#	critical points: $(m_1, m_2, \gamma_1, \gamma_2, \gamma_3)$
D_1		$k_1 > b_1$	0	
D_2	$k_2 < b_2$	$\Delta > 0$ $k_1/b_1 + k_2/b_2 > 1, k_1 < b_1$	8	$((-1)^k \Lambda_1^+, (-1)^l \Lambda_2^+, (-1)^i \Gamma_1^+, (-1)^j \Gamma_2^+, 0)$
D_3		$k_1/b_1 + k_2/b_2 < 1$	0	
D_4^3		$k_1 < b_1, k_1 + k_2 > 2b_1$	0	
D_5		$\Delta > 0$ $k_1 > b_1$	8	$((-1)^k \Lambda_1^-, (-1)^l \Lambda_2^-, (-1)^i \Gamma_1^-, (-1)^j \Gamma_2^-, 0)$
$D_4^1 \cup D_4^2$	$k_2 > b_2$	$k_1 < b_1, k_1 + k_2 < 2b_1$	16	$((-1)^k \Lambda_1^\pm, (-1)^l \Lambda_2^\pm, (-1)^i \Gamma_1^\pm, (-1)^j \Gamma_2^\pm, 0)$
C_1		$\Delta = 0$ $k_1 + k_2 < 2b_1$	8	$((-1)^k \Lambda_1, (-1)^l \Lambda_2, (-1)^i \Gamma_1, (-1)^j \Gamma_2, 0)$
C_2		$\Delta = 0$ $k_1 + k_2 > 2b_1$	0	
D_4^4		$\Delta < 0$	0	

TABLE 2. Critical points for $b_1 > b_2$. Here $ijk \in \{0, 1\}$ and $l = i + k - j$.

4.4. Classification of Critical points. Given the explicit computation of all the critical points on the smooth level surfaces, we can now classify all of them. Recall that the level surface S_k is defined by (2.2). The tangent plane at $p \in S_k$ is the kernel of the matrix (3.1) formed by the gradients of the defining equations. Let $p = (m_1, m_2, \gamma_1, \gamma_2, \gamma_3)$ be a critical point of the flow, then $\gamma_3 = 0$ and none of the other coordinates vanishes. Thus, near a critical point p we have a local frame of the tangent space \mathcal{B}_k given by

$$v_1 = \frac{b_1 \gamma_3}{m_1} \frac{\partial}{\partial n_1} - \frac{\gamma_3}{\gamma_1} \frac{\partial}{\partial n_1} + \frac{\partial}{\partial n_3} \text{ and } v_2 = \frac{b_1 \gamma_2}{m_1} \frac{\partial}{\partial n_1} - \frac{b_2 \gamma_2}{m_2} \frac{\partial}{\partial n_2} - \frac{\gamma_2}{\gamma_1} \frac{\partial}{\partial n_1} + \frac{\partial}{\partial n_2}$$

We see that integral curves of v_1 are given by $\gamma_2 \equiv \mathbf{b}$ and the integral curves of v_2 are given by $\gamma_3 \equiv \mathbf{b}$. In particular, $\{\gamma_2, \gamma_3\}$ defines a local coordinate chart around p . By an abuse of notation, we may write

$$v_1 = \partial_{\gamma_3} \text{ and } v_2 = \partial_{\gamma_2}$$

Then the Suslov vector field on S_k near p can be written as

$$X = (\gamma_2 m_2 - \gamma_1 m_1) \partial_{\gamma_3} - m_2 \gamma_3 \partial_{\gamma_2}$$

Let P be a critical point of X and suppose that $\gamma_2(P) = c$ and $\gamma_3(P) = 0$. From the equations (2.2), we compute that the linearization of X at P to be

$$(4.4) \quad \left(m_2(P) - \frac{b_2 \gamma_2(P)^2}{m_2(P)} + \frac{m_1(P) \gamma_2(P)}{\gamma_1(P)} - \frac{b_1 \gamma_1(P) \gamma_2(P)}{m_1(P)} \right) (\gamma_2 - c) \partial_{\gamma_3} - m_2(P) \gamma_3 \partial_{\gamma_2}$$

which gives the Jacobian of X at P :

$$J_X(P) = \begin{pmatrix} 0 & -m_2(P) \\ m_2(P) - \frac{b_2 \gamma_2(P)^2}{m_2(P)} + \frac{m_1(P) \gamma_2(P)}{\gamma_1(P)} - \frac{b_1 \gamma_1(P) \gamma_2(P)}{m_1(P)} & 0 \end{pmatrix}$$

The characteristic polynomial of $J_X(P)$ is

$$\lambda^2 - m_2(P) \left(m_2(P) - \frac{b_2 \gamma_2(P)^2}{m_2(P)} + \frac{m_1(P) \gamma_2(P)}{\gamma_1(P)} - \frac{b_1 \gamma_1(P) \gamma_2(P)}{m_1(P)} \right)$$

which simplifies to

$$(4.5) \quad \lambda^2 + k_1 + k_2 - 2(m_1(P)^2 + m_2(P)^2)$$

since at P , we have $\gamma_2(P)m_2(P) - \gamma_1(P)m_1(P) = 0$. The type of the singularity is determined by the roots of the characteristic polynomial in (4.5).

First consider the case where $b_1 = b_2 = b$. In this case, the flow has 8 critical points on the level set S_k when $(k_1, k_2) \in D_2 \cup D_5$, and no critical points in other regions.

Proposition 4.3. *When $b_1 = b_2 = b$, the critical points on S_k are all saddles if $k \in D_2$, and are all centers if $k \in D_5$.*

Proof. In this case, the explicit coordinates for the singular points in Table 1 lead to

$$m_1(P)^2 + m_2(P)^2 = k_1 + k_2 - b$$

which implies that the roots of the characteristic polynomial is given by

$$\pm \sqrt{2b - (k_1 + k_2)}$$

The statement follows noticing that $k_1 + k_2 < 2b$ in D_2 , while $k_1 + k_2 > 2b$ in D_5 . \square

Next, consider $b_1 \neq b_2$. Without loss of generality, we suppose that $b_1 > b_2$.

Proposition 4.4. *Suppose that $b_1 > b_2$. When S_k is a smooth 2-manifold, we have:*

- If $(k_1, k_2) \in D_2$ then the 8 critical points are all saddles.
- If $(k_1, k_2) \in D_4^1 \cup D_4^2$ then there are 8 centers and 8 saddles.
- If $(k_1, k_2) \in D_5$ then the 8 critical points are all centers.
- If $(k_1, k_2) \in C_1$ then there are 8 non-hyperbolic critical points.

Proof. Using (2.2) and the fact that $\gamma_3(P) = 0$ at critical point P , we see that

$$m_1(P)^2 + m_2(P)^2 = k_1 + k_2 - b_2 - (b_1 - b_2)\gamma_1(P)^2$$

Thus (4.5) becomes

$$\lambda^2 - 2(b_1 - b_2) \left[\frac{k_1 + k_2 - 2b_2}{2(b_1 - b_2)} - \gamma_1(P)^2 \right]$$

When $\Delta \neq 0$, the critical points are non-degenerate. Let's call the critical points of the form $((-1)^i \Gamma_1^+, (-1)^j \Gamma_2^+, (-1)^k \Lambda_1^+, (-1)^l \Lambda_2^+)$ the *+critical points*, and the critical points of the form $((-1)^i \Gamma_1^-, (-1)^j \Gamma_2^-, (-1)^k \Lambda_1^-, (-1)^l \Lambda_2^-)$ the *--critical points*. At the \pm -critical points, by (4.3), (4.5) further simplifies to

$$\lambda^2 \mp \sqrt{\Delta}, \text{ respectively}$$

In particular, all +-critical points are saddles and --critical points are centers. This gives the first three statements.

When $(k_1, k_2) \in C_1$, we have $\Delta = 0$ at the critical points and they are all degenerate. The linearization (4.4) of X at a critical point P here becomes

$$(4.6) \quad -m_2(P)\gamma_3\partial_{\gamma_2} \text{ with } m_2(P) \neq 0$$

which implies that they are nonhyperbolic. \square

4.5. Periodic orbits. Recall that on each level surface S_k , an orbit of the Suslov flow projects to a portion of an orbit of a linear flow on the torus and the critical points of the Suslov flow correspond to precisely the points where \mathcal{D}_k is tangent to the linear flow. Thus a generic orbit of the flow does not contain any critical point in its closure, and we say such generic orbits *non-critical*.

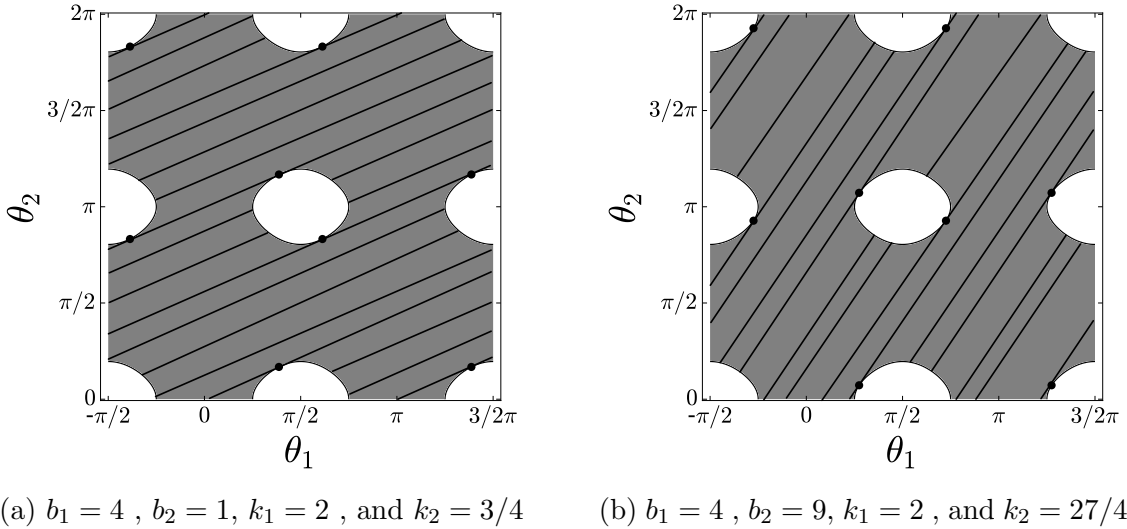


FIGURE 6. The flow for $k \in D_2$, for two different values of k .

Figures 6 and 7 illustrate the projection of the Suslov flow when $k \in D_2$ and $k \in D_4$, respectively. We notice that Figure 7a corresponds to $k \in D_4^4$, where there is no critical

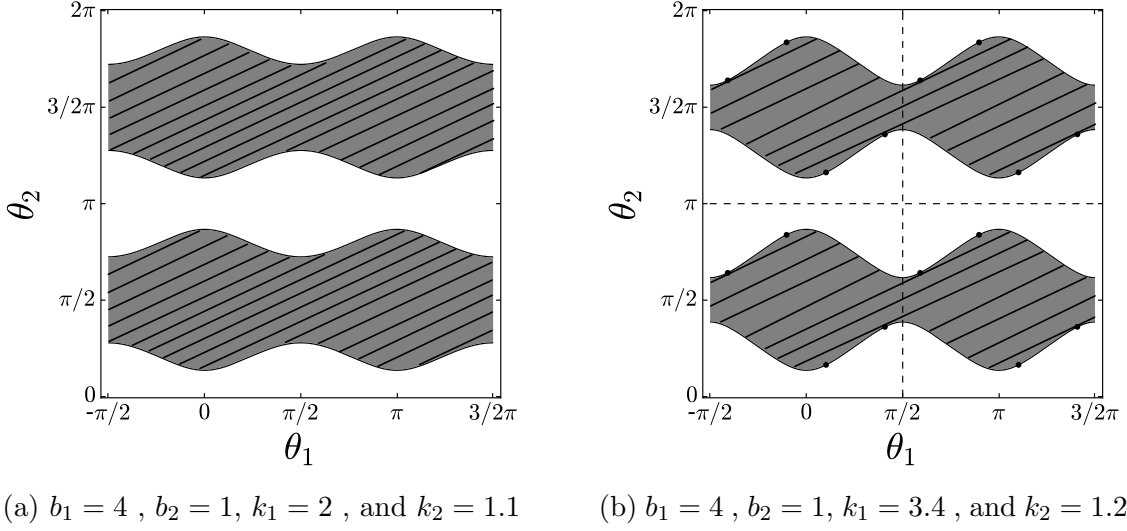


FIGURE 7. The flow for $k \in D_4$, for two different values of k .

point, while Figure 7b corresponds to $k \in D_4^1 \cup D_4^2$. One can understand the periodicity of the Suslov orbits from these projections.

Lemma 4.5. *Let \mathcal{O} be a non-critical orbit of the Suslov flow on the level set S_k and \mathcal{O}_T its projection to the torus. If $\mathcal{O}_T \cap \mathcal{D}_k$ contains at least 2 points, then \mathcal{O} is periodic.*

Proof. Let $pq \in \mathcal{O}_T \cap \mathcal{D}_k$ and let ℓ be the component of \mathcal{O}_T such that $\mathcal{D} = \{pq\}$. By Lemma 3.3, we see that $(\varphi_k \circ p_k)^{-1}(\ell) \cong S^1$. Since \mathcal{O} is connected, we see that $\mathcal{O} \cong S^1$, i.e. it is periodic. \square

From the proof, we also see that the torus projection of the closure of a Suslov orbit can have at most two intersection points with \mathcal{D}_k . The following proposition states that in a large open set of the configuration space, Suslov orbits are generically periodic.

Proposition 4.6. *Let $Q_1 = \cup_{k \notin \overline{D_1}} S_k$. Then Suslov orbits in Q_1 are generically periodic.*

Proof. Suppose that $\sqrt{\frac{b_2}{b_1}} \in \mathbb{Q}$, then the corresponding linear flow on T^2 are periodic. Let \mathcal{O} be a Suslov orbit on an smooth level surface S_k , then it may not be periodic only if its torus projection \mathcal{O}_T contains a critical point in its closure. There is a finite number of those non-periodic orbits on each level surface, which implies that generic Suslov orbits are periodic. Note that in this case, we do not have to restrict to Q_1 .

Suppose that $\sqrt{\frac{b_2}{b_1}} \notin \mathbb{Q}$, then the corresponding linear flow on T^2 are not periodic and we restrict the consideration to $k \in Q_1$. For such k , $\mathcal{D}_k \neq \emptyset$, and $T^2 \setminus U_k$ is an open subset. Any orbit of the corresponding linear flow is dense in T^2 , and intersects \mathcal{D}_k infinitely many times. Since there are only finitely many critical points on each level surface S_k , there are only finitely many linear orbits on T^2 that intersect with the torus projection of the critical points. By Lemma 4.5 all the Suslov orbits are periodic, except for a finite number which connects critical points. \square

We remark that when there is no critical point on a level surface in Q_1 , e.g. $k \in D_4^4$, all Suslov orbits on such S_k are periodic. Furthermore, when a Suslov orbit is not periodic, it can be either homoclinic or heteroclinic, e.g. Figure 6a depicts 4 heteroclinic orbits and 8 homoclinic orbits, while in Figure 7b there are 16 homoclinic orbits.

4.6. Topology of the level surfaces S_k via the Poincaré-Hopf theorem. The Poincaré-Hopf theorem [5] provides a deep link between a purely analytic concept, namely the index of a vector field, and a purely topological one, that is, the Euler characteristic. Recall that the Euler characteristic of a compact connected orientable two dimensional manifold is given by

$$\mathcal{X} = 2 - 2g$$

where g is the genus, that is the number of “holes”, and that such manifold is determined, up to an homeomorphism, by its genus. The Poincaré-Hopf theorem allows us to determine the topology of M by counting the indices of the zeroes of a vector field on M .

Theorem 4.7 (Poincaré-Hopf). *Let M be a compact manifold and let v be a smooth vector field on M with isolated zeroes. If M has a boundary, then v is required to point outward at all boundary points. Then, the sum of the indices at the zeroes of such vector fields is equal to the Euler characteristic of M , that is, we have*

$$\mathcal{X}(M) = \sum_i \text{index}_{x_i}(v).$$

We now use the Poincaré-Hopf theorem to give an alternative proof of Proposition 3.5. Since on a compact two manifold the index of a sink, a source, or a center is +1, and the index of a hyperbolic saddle point is -1 , the classification of the critical points given in Proposition 4.4 together with the knowledge of the number of connected components of the manifolds gives the proof for $\Delta \neq 0$. For instance, if $k \in D_2$, then there are 8 saddle points, so that $\mathcal{X}(S_k) = -8$, and $g = \frac{2-\mathcal{X}}{2} = 5$. If $\Delta = 0$, the critical points are all degenerate and the vector field near the critical points is given by (4.6). In this case it is easy to see that the index of any critical point is 0, and thus $\mathcal{X}(S_k) = 0$. Since there are two connected components $g = 1$ on each of them. It follows that S_k is isomorphic to two copies of T^2 .

In [2] a similar approach was used to obtain the topology of Suslov’s problem. The main difference is that the authors used an extension of the Poincaré-Hopf theorem that applies to compact manifolds with boundary even when the vector field does not point outward at all boundary points.

5. PHYSICAL MOTION

5.1. Poisson sphere. The 2-sphere $\gamma_1^2 + \gamma_2^2 + \gamma_3^2 = 1$ is known as the *Poisson sphere*. Let π be the projection of S_k onto the Poisson sphere. The *domain of possible motion* (DPM) corresponding to $k \in \mathbb{R}^2$ is the set $P_k = \pi(S_k) \subset S^2$, that is, it is the image of the projection of S_k to the Poisson sphere [3]. If $p \in S^2$ is a point on the Poisson sphere, a vector $v \in \mathbb{R}^2$ such that $(pv) \in S_k$ is said to be an *admissible velocity* at the point $p \in S^2$. A classification of the possible types of DPMs together with a study

of the set of admissible velocities gives a topological and geometrical description of the mechanical system and it is useful in describing the main features of the physical motion for various values of k . We rewrite the equations as

$$(1) \quad \gamma_1^2 = \frac{1}{b_1}(k_1 - m_1^2),$$

$$(2) \quad \gamma_2^2 = \frac{1}{b_2}(k_2 - m_2^2)$$

and $\gamma_3^2 = 1 - \gamma_1^2 - \gamma_2^2$. The cardinality of the preimage of a point $x = (\gamma_1, \gamma_2, \gamma_3) \in S_k$ is given by the number of pairs of (m_1, m_2) that satisfy the equations (1) and (2) above. Then $x \in P_k$ iff

$$\gamma_1^2 \leq \frac{k_1}{b_1} \text{ and } \gamma_2^2 \leq \frac{k_2}{b_2}$$

or equivalently we have

$$(5.1) \quad P_k = \{\gamma_1^2 + \gamma_2^2 + \gamma_3^2 = 1\} \cap \left\{ (\gamma_1, \gamma_2, \gamma_3) \in \left[-\sqrt{\frac{k_1}{b_1}}, \sqrt{\frac{k_1}{b_1}} \right] \times \left[-\sqrt{\frac{k_2}{b_2}}, \sqrt{\frac{k_2}{b_2}} \right] \times \mathbb{R} \right\}$$

In the interior of P_k , we have $m_1 \neq 0$ and $m_2 \neq 0$, which implies that the projection $S_k \rightarrow P_k$ is 4-to-1 in the interior.

The region P_k may have boundary components, over which one or both of m_1 and m_2 vanish. If exactly one of m_1 and m_2 vanishes, the projection is 2-to-1. If $m_1 = 0$, then $\dot{\gamma}_1 = 0$, and if $m_2 = 0$, then $\gamma_2 = 0$. In the case $m_1 = m_2 = 0$, the corresponding points in P_k are corners and the projection is 1-to-1 and $\dot{\gamma}_1 = \dot{\gamma}_2 = \dot{\gamma}_3 = 0$. The diagrams below illustrates the regions P_k for various values of k .

Clear pictures emerge when the observations so far are combined. By (5.1), the image P_k of S_k on the Poisson sphere is bounded by

$$\gamma_1 = \pm \sqrt{\frac{k_1}{b_1}} \text{ and } \gamma_2 = \pm \sqrt{\frac{k_2}{b_2}}$$

which correspond precisely to the following lines on the flat torus T^2 , as indicated by the dashed lines in Figure 3:

$$\theta_1 = \pm \frac{\pi}{2} \text{ and } \theta_2 = 0 \text{ or } \pi$$

The dashed lines divide T^2 into four components, and the projection $\pi : S_k \rightarrow P_k$ restricted to each component is 1-to-1; and the image of shaded region contained in each of the components coincide. The following proposition provides a detailed classification of the DPM for various values of $k \in \mathbb{R}^2$.

Proposition 5.1. *Over the interior of the domain of possible motion P_k , the projection $\pi : S_k \rightarrow P_k$ is 4-to-1. On the boundary components of P_k , the projection is 2-to-1, except for over the corners when $k \in D_1$, where it is 1-to-1. Moreover, we have*

- (1) *For $k \in D_1$, each torus in S_k is projected onto a component of P_k . Each component of P_k is a square, see figure 8(1).*
- (2) *For $k \in D_2$ the set P_k is a sphere with four holes as depicted in figure 8(2).*

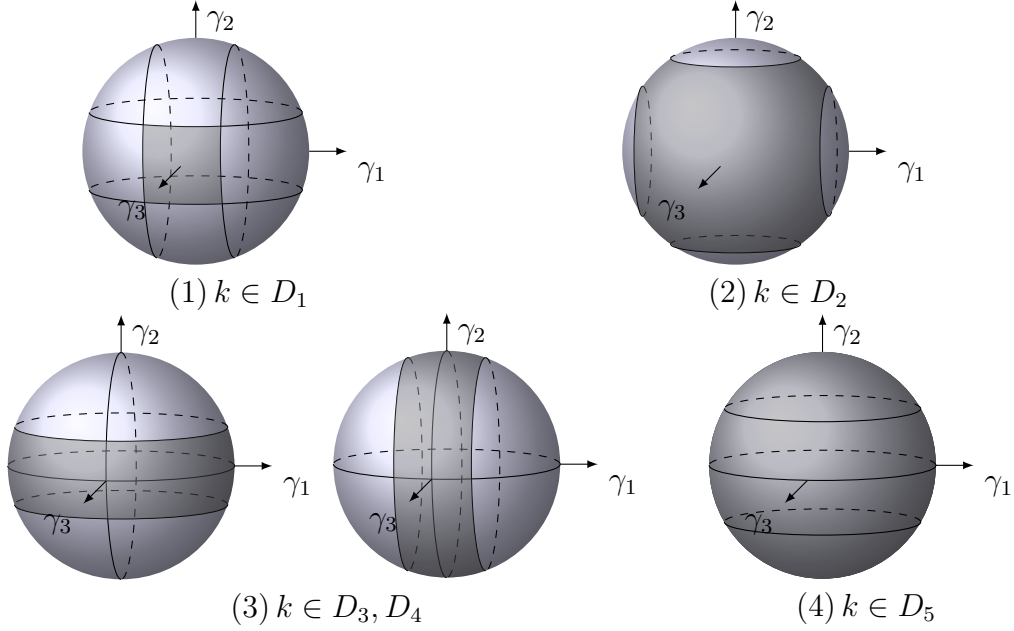


FIGURE 8. The domain of possible motion P_k for various values of k . (1) For $k \in D_1$, P_k has the form of two squares on opposite sides of the Poisson sphere. (2) For $k \in D_2$, P_k is a sphere with four holes. (3) For $k \in D_3, D_4$, P_k is a horizontal or vertical band wrapping around the sphere. (4) For $k \in D_5$, P_k is the whole sphere.

- (3) For $k \in D_3$ or D_4 , the projection π restricted to each torus component of S_k is 2-to-1 in the interior of P_k . P_k is a band wrapping around the Poisson sphere, see figure 8(3).
- (4) For $k \in D_5$, the projection π is an isomorphism when restricted to each S^2 -component of S_k , see figure 8(4).

We can now use Proposition 5.1 to understand the physical motion of the rigid body.

If $k \in D_1$, the trajectories in each component of P_k , are similar to Lissajous figures (the sum of independent horizontal and vertical oscillations). For each point inside each square there are four admissible velocities, there are two on its sides and one on the vertices. If $\sqrt{\frac{b_2}{b_1}} \notin \mathbb{Q}$, then the trajectories is dense in the squares, otherwise they are periodic. In either case \mathbf{E}_3 wobbles around the vertical direction, while \mathbf{E}_1 remains close to horizontal and the wheels remain close to being vertical (see figure 1).

If $k \in D_2$, almost all the trajectories are periodic except for a finite number of orbits which connect critical points. For points in the interior of P_k there are four admissible velocities. There are two admissible velocities on the boundary of P_k . This means that there are two trajectories for each point in the interior of P_k and each trajectory can be followed in either direction. The physical motion in this case can be distinguished from the previous case since \mathbf{E}_3 can go from pointing upward to pointing downward.

If $k \in D_3$, the trajectories are confined in a band wrapping around the sphere and alternatively touch the upper and the lower boundary of the band. Since this region is

the image of two tori there are two admissible velocities at each point, and a point can move along the trajectories in either direction. In this case \mathbf{E}_3 performs a complete revolution wobbling about the vertical plane spanned by \mathbf{e}_1 and \mathbf{e}_3 . The wheels remain close to vertical (see Figure 1). The case $k \in D_4$ is similar. When $b_1 > b_2$, certain subregions of D_4 allow homoclinic or heteroclinic orbits. From Figure 7b, we see that in this case, the behaviour of periodic orbits changes drastically on either side of a homoclinic or heteroclinic orbit.

If $k \in D_5$, the trajectories are homeomorphic to circles. In this case there are four possible velocities for each point on P_k . It follows that there are two trajectories for each point on the Poisson sphere and each trajectory can be followed in either direction.

ACKNOWLEDGEMENTS

The authors wish to express their appreciation for helpful discussions with Luis Garcia-Naranjo and Dmitry Zenkov. The research was supported in part by Natural Sciences and Engineering Research Council of Canada (NSERC) Discovery Grants (SH, MS).

REFERENCES

1. Yuri N Fedorov and Božidar Jovanović, *Quasi-Chaplygin systems and nonholonomic rigid body dynamics*, Letters in Mathematical Physics **76** (2006), no. 2, 215–230.
2. Oscar E Fernandez, Anthony M Bloch, and Dmitry V Zenkov, *The geometry and integrability of the Suslov problem*, Journal of Mathematical Physics **55** (2014), no. 11, 112704.
3. Anatolij T Fomenko, *Visual geometry and topology*, Springer Science & Business Media, 2012.
4. Valerii Vasil'evich Kozlov, *On the integration theory of equations of nonholonomic mechanics*, Regular and Chaotic Dynamics **7** (2002), no. 2, 161–176.
5. John Willard Milnor, *Topology from the Differentiable Viewpoint*, Princeton University Press, 1997 (en).
6. GK Suslov, *Theoretical mechanics*, Gostekhizdat, Moscow **3** (1946), 40–43.
7. Ya V Tatarinov, *Construction of non-torical invariant manifolds in a certain integrable nonholonomic problem*, Usp. Mat. Nauk **40** (1985), no. 5, 216 (russian).
8. ———, *Separation of variables and new topological phenomena in holonomic and nonholonomic systems*, Trudy Seminara po Vekt. i Tenz. Anal. **23** (1988), 160–174 (russian).
9. V Wagner, *On the geometrical interpretation of the motion of nonholonomic dynamical systems*, Trudy Seminara po Vekt. i Tenz. Anal. **23** (1941), no. 5, 301–327 (russian).